Brief Communication

MOLECULAR METABOLISM

Imaging adipose tissue browning using the TSPO-18kDa tracer [^{18}F]FEPPA

S.V. Hartimath [1], S. Khanapur [1], R. Boominathan [1], L. Jiang [1], P. Cheng [1], F.F. Yong [1], P.W. Tan [1], E.G. Robins [1,2], J.L. Goggi [1,*]

ABSTRACT

Objectives: The browning of white adipose tissue (WAT) into beige has been proposed as a strategy to enhance energy expenditure to combat the growing epidemic of obesity. Research into browning strategies are hampered by the lack of sensitive, translatable, imaging tools capable of detecting beige fat mass non-invasively. [^{18}F]FDG is able to detect activated beige fat but provides little information on unstimulated beige fat mass. We have assessed the use of [^{18}F]FEPPA, a tracer for the TSPO-18KDa found on the outer mitochondrial membrane, as an alternative imaging agent capable of detecting unstimulated brown fat (BAT) and beige fat.

Methods: Female Balb/c mice (n = 5) were treated for 7 days with the β3 adrenergic agonist CL-316,243 to induce the browning of inguinal WAT (beige fat). Animals were imaged longitudinally with [^{18}F]FDG and [^{18}F]FEPPA and uptake in interscapular BAT and inguinal WAT assessed. The browning of inguinal WAT was confirmed using H&E and immunohistochemical detection of UCP-1 and TSPO.

Results: Repeated dosing with β3-adrenergic agonist CL-316,243 caused a significant increase in [^{18}F]FDG uptake in both interscapular BAT and inguinal WAT associated with the increased metabolic activity of brown and beige adipocytes respectively. [^{18}F]FEPPA uptake was likewise increased in inguinal WAT but showed no increase in BAT uptake due to stimulation over the same time course. Furthermore, inguinal WAT uptake was unaffected by pharmacological blockade, indicating that [^{18}F]FEPPA uptake is associated with the expression of mitochondria in BAT and beige adipocytes and independent of activation.

Conclusion: These data show that [^{18}F]FEPPA can detect BAT and newly formed beige fat under non-stimulated, thermoneutral conditions and that uptake after stimulation is linked to mitochondrial expression as opposed to activation.

Keywords Brown fat; Beige; β3-adrenergic receptor; FDG; TSPO-18kDa; PET imaging

1. INTRODUCTION

Metabolically active brown adipose tissue (BAT) plays a significant role in metabolism and energy regulation [1–3]. While white adipose tissue (WAT) is responsible for energy storage, BAT is responsible for dissipating energy through the action of the uncoupling protein-1 (UCP1). In adults, increased BAT mass has been linked to lower body mass index leading to interest in the generation of *de novo* BAT as a potential therapeutic approach for obesity. Chemical stimulation with β3-adrenergic receptor (β3AR) agonists has been shown to induce browning in WAT but determination of the quantity and location of this new beige fat mass is a challenge [4]. Numerous imaging approaches have attempted to detect BAT [5] including magnetic resonance imaging (MRI), which relies on the unique chemical-shift of water-fat signals due to differences in morphology and chemical composition between WAT and BAT [6,7]. However, reliable localization and quantification of beige tissue mass are hampered by poor sensitivity as the newly brown adipocytes are interspersed in WAT. Positron emission tomography (PET) is a uniquely sensitive imaging method and numerous tracers have been assessed for their ability to quantify BAT. [^{18}F]FDG imaging is the current gold standard for imaging BAT and has been used to image beige fat, but detection is variable and dependent on stimulation through cold exposure or chemical stimulation [8,9]. Other PET radiopharmaceuticals have been developed to quantify BAT mass including the cannabinoid receptor 1 imaging agent [^{18}F]FMPEP, the noradrenaline transporter agent [^{11}C]MRB, and the noradrenaline analogue [^{11}C]MHED; however, they have not been assessed for the ability to measure beige fat *in vivo* under unstimulated or thermoneutral conditions [10–13]. Both brown adipocytes and beige adipocytes have multilocular lipid droplets and possess abundant mitochondria that express UCP1 [14] whereas the surrounding white adipocytes only have one large lipid droplet and a relative paucity of mitochondria [13,15]. This difference in mitochondrial abundance between WAT and beige fat suggests that an imaging agent able to quantify mitochondrial expression may be ideal for identifying beige fat mass. TSPO-18kDa (TSPO) is a five transmembrane domain protein located on the outer membrane of mitochondria and numerous radiopharmaceuticals have been developed to image TSPO expression, primarily for neuroinflammatory imaging [16]. Preclinical studies have shown that TSPO tracers can image BAT *in vivo* [17] and the TSPO

[1]Singapore Bioimaging Consortium, Agency for Science, Technology and Research (A* STAR), 11 Biopolis Way, #07-10, Helios, 138667, Singapore [2]Clinical Imaging Research Centre, Yong Loo Lin School of Medicine, National University of Singapore, 117599, Singapore

*Corresponding author. Fax: +65 6478 8908. E-mail: julian_goggi@sbic.a-star.edu.sg (J.L. Goggi).

Received March 21, 2019 • Revision received April 26, 2019 • Accepted May 2, 2019 • Available online 6 May 2019

https://doi.org/10.1016/j.molmet.2019.05.003

tracer [^{11}C]PBR28 has already been shown to identify BAT mass clinically [18]. The current study, however, is the first to attempt to use a TSPO tracer to detect the development of new beige fat deposits in WAT after β3AR agonist stimulation.

2. MATERIALS AND METHODS

No-carrier-added aqueous [^{18}F]fluoride ion was produced *via* the [^{18}O(p,n)^{18}F] nuclear reaction (GE PETtrace 860 cyclotron). The compounds 2- (2- ((N-(4-phenoxypyridin-3-yl)acetamido)methyl)phenoxy) ethyl-4-methylbenzenesulfonate (FEPPA precursor, catalogue number 1654) and N-(2-(2-Fluoroethoxy)benzyl)-N-(4-phenoxypyridin-3-yl) acetamide (FEPPA reference standard, catalogue number 1655) were purchased from ABX GmbH, Germany. Acetonitrile (99.8%), anhydrous potassium carbonate (99.99%), 4,7,13,16,21,24-hexaoxa-1,10-diazabicyclo[8.8.8]hexacosane (Kryptofix®222, 98%), phosphoric acid 85 wt% in H_2O (99.99%), and sodium bicarbonate (≥99.7%) were procured from Sigma—Aldrich Pte Ltd. HPLC-grade acetonitrile and Millex GV 0.22 μm filters were purchased from Merck Pte. Ltd. and 0.9% wt saline solution was purchased from Braun Medical Industries and used as supplied.

All reactions were carried out in closed Thermo Scientific™ conical reacti-vial™ (5 ml capacity). Sep-Pak® light (46 mg) Accell™ plus QMA carbonate was purchased from Waters Corporation and pre-conditioned with 10 ml deionized water (Elga Purelab Flex3, 18.2 MΩ cm) before use. Radiochemical isolation and purification was conducted by semi-preparative radio-HPLC system comprising of two Knaur Smartline 1050 pumps, Manual injection valve (6-port/3-channel), SmartMix 100 solvent mixer, Smartline UV-Detector 2520 (λ = 254 nm) and Flow-Count radio-HPLC NaI detection system. Quality control analytical radio-HPLC was performed on a UFLC Shimadzu HPLC system equipped with a dual wavelength UV detector and a NaI/PMT-radio detector (Flow-Ram, LabLogic). Radioactivity measurements were made with a CRC-55tPET dose calibrator (Capintec, USA).

2.1. Radiochemistry

N-(2-(2-[^{18}F]Fluoroethoxy)benzyl)-N-(4-phenoxypyridin-3-yl)acetamide ([^{18}F]FEPPA) was synthesized using a method adapted from those previously reported [16,19]. Aqueous [^{18}F]fluoride (typically 7 GBq in *ca.* 2.5 ml) was trapped on a preconditioned Sep-Pak® light (46 mg) Accell™ plus QMA carbonate (Waters). The trapped [^{18}F] fluoride anion was eluted into the reaction vial using 1 ml of a 96: 4 (v/v) acetonitrile: water mixture containing K_2CO_3 (3 mg, 21.7 μmol) and Kryptofix 222 (14.5 mg, 38.5 μmol). The $[K(K_{222})]^+[^{18}F]F^-$ complex was azeotropically dried under a stream of nitrogen gas (250 ml/min) at 90 °C with the addition of 1 × 0.5 ml anhydrous acetonitrile. After cooling, a solution of the tosyl-precursor (5 mg, 9.4 μmol) in anhydrous acetonitrile (0.7 ml) was added before the reaction vial was sealed and heated at 90 °C for a further 10 min. After cooling to room temperature, the crude reaction mixture was diluted with 3 ml HPLC mobile phase (30/70 v/v ethanol/0.1% phosphoric acid in water) and subjected to purification by isocratic semi-preparative radio-HPLC (Nucleodur pyramid C18, 5μ, 110 Å, 250 × 10 mm; 30/70 v/v ethanol/0.1% phosphoric acid in water; 5 mL/min, λ = 254 nm). The [^{18}F] FEPPA fraction was isolated with a retention time of between 13.5 and 13.7 min, neutralized with 10% sodium bicarbonate solution (1 ml) and diluted to 10 ml with 0.9% w/v saline before filtration through 0.22 μm Millex GV filter to afford the final product. [^{18}F]FEPPA was prepared with a non-decay corrected radiochemical yield of 40 ± 7% within 50—60 min (n = 12) from aqueous [^{18}F]fluoride. The radiochemical purity was greater than 99% and molar activity was 114 ± 54 GBq/μmol at the end of the synthesis. The radiochemical identity of the [^{18}F] FEPPA was confirmed by co-elution of the product with an authentic sample of [^{19}F]FEPPA using analytical radio-HPLC (Shim-pack GIST C18, 5 μ, 100 Å, 250 mm × 4.6 mm column, water: acetonitrile gradient elution 0.01—0.20 min 10% acetonitrile, 0.20—6.00 min 10—95% acetonitrile, 6.00—10.00 min 95—10% acetonitrile, flow rate of 2 ml/min, λ = 254 nm). The retention time of authentic [^{19}F] FEPPA and [^{18}F]FEPPA was 6 min. The solution stability of formulated [^{18}F]FEPPA was assessed over 7.5 h at room temperature (n = 2) during which time no change in radiochemical purity was observed.

2.2. Animal procedures

Animal procedures were carried out in accordance with the Institutional Animal Care and Use Committee Singapore. BALB/c mice aged 6—8 weeks were purchased from In Vivos Singapore, kept at room temperature with a 12-hour light—dark cycle and had free access to food and water. Saline or β3-adrenergic receptor agonist CL-316,243 compound (1 mg/kg) was administered intraperitoneally daily for 7 days. β3-adrenergic receptor antagonist L-748,328 (1 mg/kg) was administered 1 h prior to imaging on Day 7 to determine basal binding.

2.3. PET-CT and MR imaging

The animals were imaged longitudinally 0, 1, 4, and 7 days after initiation of treatment using the Siemens Inveon PET-CT and the Mediso nanoscan 3T MR system using a modified version of the methodology described by Wang et al. [20]. Briefly, animals were imaged one hour after dosing with either CL-316,243 or vehicle, anesthetized using inhalational isoflurane anesthesia (maintained at 1.5% alveolar concentration) and injected with either [^{18}F]FDG or ^{18}F] FEPPA (∼10 MBq per animal) *via* the lateral tail vein. They were maintained heated and anaesthetized throughout the procedure. Static PET acquisitions were performed at 60—80 min post-injection and CT and T2 weighted fast spin echo MR scans were used to delineate fat depots (TR 3843 ms, TE 87.5 ms, matrix size 256 × 256, 50.0 mm FOV, 1.0 mm slice thickness with no slice gap acquisition time 9 min). Animals were monitored for maintenance of body temperature and respiration rate during imaging studies using the Biovet physiological monitoring system. Post-analysis of reconstructed calibrated images were performed with FIJI and Amide software (version 10.3 Sourceforge). Uptake of radioactivity in the fat depots was determined by the placement of a volume of interest (VOI) around the interscapular BAT and inguinal WAT regions as delineated by CT and MR imaging. A VOI was also placed in the quadriceps muscle to provide reference tissue values.

2.4. Histology

On day 7, the inguinal fat tissues were dissected and fixed with 10% formalin, embedded in paraffin and sectioned. Sections were stained with hematoxylin and eosin (H&E) or were probed with an antibody for UCP1 (1:100, ab23841, Abcam) or TSPO-18kDa (1:100, ab109497, Abcam).

2.5. Statistical analysis

A two-way ANOVA with multiple Bonferroni post-test was performed using GraphPad Prism version 8.0.0 for Windows, GraphPad Software, San Diego, California USA, www.graphpad.com, $p < 0.05$ was considered statistically significant. Data are expressed as mean and error bars are expressed as ± SD.

3. RESULTS

3.1. Quantification of inguinal adipose browning with [^{18}F]FDG and [^{18}F]FEPPA PET imaging

PET imaging combined with CT was performed on days 0, 1, 4, and 7 post dosing with CL-316,243. As seen in Figure 1B, the retention of both [^{18}F]FDG and [^{18}F]FEPPA in inguinal WAT was significantly increased after subchronic treatment with CL-316,243.

On Day 1, CL-316,243 treatment had no significant effect on retention of [^{18}F]FDG (1.6 $\pm$ 0.6% ID/g) compared to vehicle treatment (1.7 $\pm$ 0.6% ID/g) nor on the retention of [^{18}F]FEPPA (3.7 $\pm$ 0.8%ID/g) compared to vehicle (2.8 $\pm$ 1.2% ID/g). By Day 4, the retention of [^{18}F]FDG was significantly increased in the CL-316,243 treated inguinal WAT (3.5 $\pm$ 1.5% ID/g compared to 1.8 $\pm$ 0.5% ID/g in the vehicle *p $=$ 0.02). Likewise, the retention of [^{18}F]FEPPA was significantly increased in the CL-316,243 treated inguinal WAT (4.9 $\pm$ 1.0% ID/g compared to 2.9 $\pm$ 0.5% ID/g in the vehicle ***p $=$ 0.004) after 4 days of treatment. Radiotracer uptake was further increased in inguinal WAT by Day 7 in the CL-316,243 treated inguinal WAT for both [^{18}F]FDG (4.4 $\pm$ 0.8% ID/g compared to 1.5 $\pm$ 0.4% ID/g in the vehicle ****p $=$ 0.0001) and [^{18}F]FEPPA (7.0 $\pm$ 1.3% ID/g compared to 2.5 $\pm$ 0.5% ID/g in the vehicle ****p $=$ 0.00009). Pretreatment with the β3AR antagonist L-748,328 had no significant effect on [^{18}F]FEPPA uptake in inguinal WAT on Day 7 (Figure 1D, 6.43 $\pm$ 0.63% ID/g).

3.2. Interscapular brown fat imaging with [^{18}F]FDG and [^{18}F]FEPPA

As seen in Figure 1C, while the retention of [^{18}F]FDG in interscapular brown fat significantly increased with CL-316,243 treatment, the uptake of [^{18}F]FEPPA remained unchanged.

On Day 1, CL-316,243 treatment had no significant effect on retention of [^{18}F]FDG (5.7 $\pm$ 2.4% ID/g) compared to vehicle treatment (4.4 $\pm$ 0.7% ID/g). By Day 4, the retention of [^{18}F]FDG was significantly increased in the CL-316,243 treated BAT (7.6 $\pm$ 1.6% ID/g compared to 4.0 $\pm$ 0.7% ID/g in the vehicle *p $=$ 0.0194) and further increased by Day 7 (16.8 $\pm$ 2.1% ID/g compared to 4.2 $\pm$ 0.4% ID/g in the vehicle ***p $=$ 0.0004). In contrast, [^{18}F]FEPPA retention was unchanged in at any of the days studied post stimulation (Day 1; 56.3 $\pm$ 17.0% ID/g in CL-treated compared to vehicle 48.8 $\pm$ 15.6% ID/g, Day 4; 56.3 $\pm$ 17.0% ID/g in CL-treated compared to vehicle 57.3 $\pm$ 8.3% ID/g and Day 7; 60.6 $\pm$ 9.9% ID/g in CL-

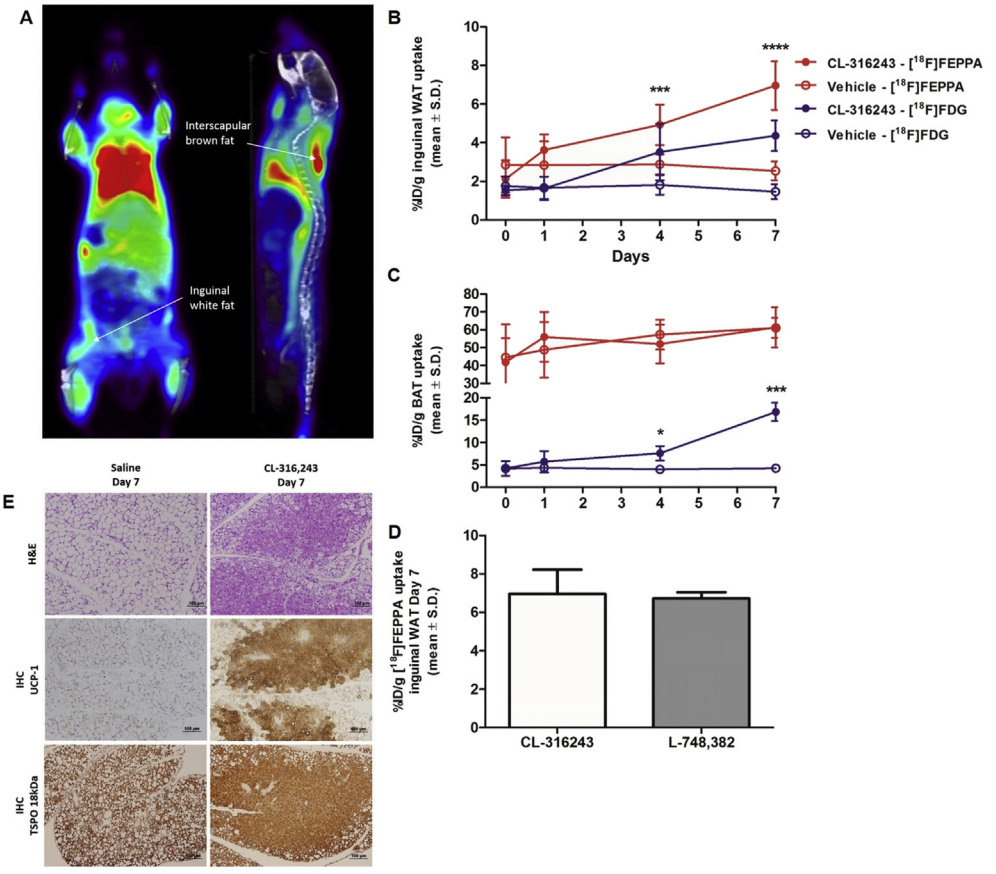

Figure 1: (A) Representative PET-CT fusion image showing retention of [^{18}F]FEPPA in inguinal WAT and interscapular BAT after 7 days of CL-316,243 treatment. (B) Graph showing retention of [^{18}F]FDG and [^{18}F]FEPPA in inguinal WAT measured by longitudinal PET imaging (~10 MBq, acquired from 60 to 80 min post injection under isoflurane anesthesia). Fat depots were delineated using CT and T2 weighted MRI. [^{18}F]FEPPA retention was significantly higher in the CL-316,243 treated inguinal fat (closed red circles) compared to the vehicle treated inguinal fat (open red circles) on days 4 and 7 post treatment. [^{18}F]FDG retention was significantly higher in the CL-316,243 treated inguinal fat (closed blue circles) compared to the vehicle treated inguinal fat (open blue circles) on days 4 and 7 post treatment. (n $=$ 5 treated and n $=$ 5 vehicle, *p $<$ 0.05, ***p $<$ 0.001, ****p $<$ 0.0001 data shown as %ID/g $\pm$ SD). (C) Graph showing retention of [^{18}F]FDG and [^{18}F]FEPPA in interscapular BAT measured by longitudinal PET. No difference in [^{18}F]FEPPA retention was observed in the CL-316,243 treated interscapular BAT (closed red circles) compared to vehicle (open red circles) at any time point. In contrast, [^{18}F]FDG retention was significantly higher in the CL-316,243 treated BAT (closed blue circles) compared to vehicle treated BAT (open blue circles) on days 4 and 7 post treatment (n $=$ 5 treated and n $=$ 5 vehicle, *p $<$ 0.05, ***p $<$ 0.001, data shown as %ID/g $\pm$ SD). (C) Bar graph showing the effect of β3AR blockade with L-748,382 on retention of [^{18}F]FEPPA in inguinal WAT after 7 days of CL-316,243 treatment (n $=$ 3, data shown as %ID/g $\pm$ SD). (D) Representative H&E (top panel) and immunohistochemical staining for UCP1 (middle panel) and TSPO-18kDa (bottom panel) in inguinal WAT sections from saline and CL-316,243-treated mice at Day 7. Scale bar, 100 μm.

treated compared to vehicle 61.0 ± 5.6% ID/g). Pretreatment with the β3AR antagonist L-748,328 to block CL-316,243 stimulation had no significant effect on [^{18}F]FEPPA uptake in interscapular BAT on Day 7 (57.5 ± 4.3% ID/g).

3.3. Histology

Histological and immunohistochemical assessment of WAT was performed after 7 days of stimulation. H&E staining clearly shows a significant increase in the presence of multilocular fat cells indicative of brown adipocyte conversion after CL-316,243 treatment compared to vehicle (Figure 1E upper panel). These findings are corroborated by immunohistochemical staining for UCP-1 (Figure 1E middle panel). IHC shows a clear increase in TSPO-18kDa expression in areas displaying staining of UCP-1 expression (Figure 1E lower panel).

4. DISCUSSION

Recently there has been a plethora of research investigating ways to enhance the expression of thermogenes in WAT. The resulting beige tissue is hypothesized to combat obesity by reducing lipids stored within WAT and increasing energy expenditure [2,3,5,21,22]. These attempts to induce beige fat necessitate the development of sensitive and specific, translatable, imaging methodologies to accurately detect beige fat mass *in vivo*. Molecular imaging probes have been assessed for their ability to quantify beige fat across the spectrum of imaging with varying degrees of success. Optical imaging techniques including endogenous contrast and near infrared dyes have proven effective in preclinical models but clinical translation is limited [9,23–25]. Clinical techniques such as MRI, skin temperature measurements, near-infrared spectroscopy, and contrast-enhanced ultrasound show the ability to accurately determine BAT mass or metabolic activity but are too insensitive to reliably detect *de novo* formation of beige fat [26,27]. PET imaging provides a uniquely sensitive method for non-invasive assessment of browning. Currently only [^{18}F]FDG uptake in stimulated beige fat has been well documented. [^{18}F]FDG uptake is linked to hexokinase 2 and UCP-1 (uncoupling protein 1) activity [9,28] providing information on the metabolic activity of the beige adipocytes but little information on the number of beige adipocytes induced by stimulation. Beige adipocyte biogenesis in WAT is induced in response to multiple external stimuli including chronic cold, exercise and β3AR agonists. These stimuli induce transdifferentiation of white adipocytes into beige adipocytes through a process involving the activation of PPARγ (peroxisome proliferator-activated receptor-γ) [29] and the PRDM16 (PRD1 domain containing protein 16) pathway [28]. Typically this conversion has been confirmed by measuring standard markers of brown adipocytes including UCP1 and mitochondrial expression. Beige adipocytes possess abundant mitochondria which express TSPO providing ample binding sites for [^{18}F]FEPPA and the surrounding white adipocytes have few mitochondria [13,15], minimizing background uptake. Furthermore, [^{18}F]FEPPA measurement of mitochondrial TSPO expression is independent of activation, as shown by the β3AR antagonist L-748,328 which had no effect on [^{18}F]FEPPA uptake in beige fat or BAT. TSPO radiopharmaceuticals seem well suited to detect beige fat mass independent of stimulation, however, this study has several limitations; firstly [^{18}F]FEPPA uptake has not been assessed in completely unstimulated beige fat as expression is transient, reverting to the white phenotype within days of withdrawal of stimulation [30]. Secondly, we are unable to quantify the proportion of [^{18}F]FEPPA uptake that may be due to non-specific binding such as the increased vascularization associated with beige fat or infiltration of macrophages which express particularly high levels of TSPO. Also β3AR stimulation is a potent inducer of beige fat, useful in preclinical models, however, clinical approaches to induce beige fat, such as cold acclimation and exercise are less potent raising the question of how sensitive a measure of unstimulated beige fat might be in humans. It is not currently understood how many white adipocytes can undergo transdifferentiation to beige adipocytes, previous studies using cold stimulation in rodents have suggested up to 50% but this may be different in humans and dependent on adipocyte population or microenvironment [29,31]. Thus further work may be necessary to evaluate [^{18}F]FEPPA for clinical use under these paradigms.

Overall, these data suggest that the TSPO tracer [^{18}F]FEPPA may be useful for detecting unstimulated beige adipocytes. As [^{18}F]FEPPA has been used to assess neuroinflammation in patients [32–34], it could potentially be repurposed to identify beige fat clinically at thermoneutral conditions.

ACKNOWLEDGMENTS

This work was supported by funding from the Singapore Bioimaging Consortium (SBIC), A*STAR, Singapore.

CONFLICT OF INTEREST

None.

APPENDIX A. SUPPLEMENTARY DATA

Supplementary data to this article can be found online at https://doi.org/10.1016/j.molmet.2019.05.003.

REFERENCES

[1] Bartelt, A., Bruns, O.T., Reimer, R., Hohenberg, H., Ittrich, H., Peldschus, K., et al., 2011. Brown adipose tissue activity controls triglyceride clearance. Nature Medicine 17(2):200–205. https://doi.org/10.1038/nm.2297. PubMed PMID: 21258337.

[2] Gunawardana, S.C., 2012. Therapeutic value of brown adipose tissue: Correcting metabolic disease through generating healthy fat. Adipocyte 1(4): 250–255. https://doi.org/10.4161/adip.21042. PubMed PMID: 23700541; PubMed Central PMCID: PMC3609108.

[3] Gunawardana, S.C., Piston, D.W., 2012. Reversal of type 1 diabetes in mice by brown adipose tissue transplant. Diabetes 61(3):674–682. https://doi.org/10.2337/db11-0510. PubMed PMID: 22315305; PubMed Central PMCID: PMC3282804.

[4] Nedergaard, J., Bengtsson, T., Cannon, B., 2007. Unexpected evidence for active brown adipose tissue in adult humans. American Journal of Physiology Endocrinology and Metabolism 293(2):E444–E452. https://doi.org/10.1152/ajpendo.00691.2006. PubMed PMID: 17473055.

[5] Symonds, M.E., Aldiss, P., Pope, M., Budge, H., 2018. Recent advances in our understanding of brown and beige adipose tissue: the good fat that keeps you healthy. F1000Research 7. https://doi.org/10.12688/f1000research.14585.1. PubMed PMID: 30079236; PubMed Central PMCID: PMC6058473.

[6] Bhanu Prakash, K.N., Verma, S.K., Yaligar, J., Goggi, J., Gopalan, V., Lee, S.S., et al., 2016. Segmentation and characterization of interscapular brown adipose tissue in rats by multi-parametric magnetic resonance imaging. Magma 29(2):277–286. https://doi.org/10.1007/s10334-015-0514-3. PubMed PMID: 26747282.

[7] Hu, H.H., 2015. Magnetic resonance of brown adipose tissue: a review of current techniques. Critical Reviews in Biomedical Engineering 43(2-3): 161–181. https://doi.org/10.1615/CritRevBiomedEng.2015014377. PubMed PMID: 27278740.

[8] Zhang, F., Hao, G., Shao, M., Nham, K., An, Y., Wang, Q., et al., 2018. An adipose tissue atlas: an image-guided identification of human-like BAT and beige depots in rodents. Cell Metabolism 27(1):252–262.e3. https://doi.org/10.1016/j.cmet.2017.12.004. PubMed PMID: 29320705; PubMed Central PMCID: PMC5764189.

[9] Chan, X.H.D., Balasundaram, G., Attia, A.B.E., Goggi, J.L., Ramasamy, B., Han, W., et al., 2018. Multimodal imaging approach to monitor browning of adipose tissue in vivo. Journal of Lipid Research 59(6):1071–1078. https://doi.org/10.1194/jlr.D083410. PubMed PMID: 29654114; PubMed Central PMCID: PMC5983400.

[10] Eriksson, O., Mikkola, K., Espes, D., Tuominen, L., Virtanen, K., Forsback, S., et al., 2015. The cannabinoid receptor-1 is an imaging biomarker of brown adipose tissue. Journal of Nuclear Medicine: Official Publication, Society of Nuclear Medicine 56(12):1937–1941. https://doi.org/10.2967/jnumed.115.156422. PubMed PMID: 26359260.

[11] Hwang, J.J., Yeckel, C.W., Gallezot, J.D., Aguiar, R.B., Ersahin, D., Gao, H., et al., 2015. Imaging human brown adipose tissue under room temperature conditions with (11)C-MRB, a selective norepinephrine transporter PET ligand. Metabolism: Clinical and Experimental 64(6):747–755. https://doi.org/10.1016/j.metabol.2015.03.001. PubMed PMID: 25798999; PubMed Central PMCID: PMC4408242.

[12] Lin, S.F., Fan, X., Yeckel, C.W., Weinzimmer, D., Mulnix, T., Gallezot, J.D., et al., 2012. Ex vivo and in vivo evaluation of the norepinephrine transporter ligand [11C]MRB for brown adipose tissue imaging. Nuclear Medicine and Biology 39(7):1081–1086. https://doi.org/10.1016/j.nucmedbio.2012.04.005. PubMed PMID: 22595487; PubMed Central PMCID: PMC4067762.

[13] Madar, I., Isoda, T., Finley, P., Angle, J., Wahl, R., 2011. 18F-fluorobenzyl triphenyl phosphonium: a noninvasive sensor of brown adipose tissue thermogenesis. Journal of Nuclear Medicine: Official Publication, Society of Nuclear Medicine 52(5):808–814. https://doi.org/10.2967/jnumed.110.084657. PubMed PMID: 21498536; PubMed Central PMCID: PMC4332805.

[14] Cinti, S., 1999. Adipose tissues and obesity. Italian Journal of Anatomy and Embryology Archivio italiano di anatomia ed embriologia 104(2):37–51. PubMed PMID: 10450668.

[15] Cedikova, M., Kripnerova, M., Dvorakova, J., Pitule, P., Grundmanova, M., Babuska, V., et al., 2016. Mitochondria in white, brown, and beige adipocytes. Stem Cells International 2016:6067349. https://doi.org/10.1155/2016/6067349. PubMed PMID: 27073398; PubMed Central PMCID: PMC4814709.

[16] Wilson, A.A., Garcia, A., Parkes, J., McCormick, P., Stephenson, K.A., Houle, S., et al., 2008. Radiosynthesis and initial evaluation of [18F]-FEPPA for PET imaging of peripheral benzodiazepine receptors. Nuclear Medicine and Biology 35(3):305–314. https://doi.org/10.1016/j.nucmedbio.2007.12.009. PubMed PMID: 18355686.

[17] Yang, J., Yang, J., Wang, L., Moore, A., Liang, S.H., Ran, C., 2017. Synthesis-free PET imaging of brown adipose tissue and TSPO via combination of disulfiram and (64)CuCl2. Scientific Reports 7(1):8298. https://doi.org/10.1038/s41598-017-09018-2. PubMed PMID: 28811616; PubMed Central PMCID: PMC5557754.

[18] Ran, C., Albrecht, D.S., Bredella, M.A., Yang, J., Yang, J., Liang, S.H., et al., 2018. PET Imaging of human brown adipose tissue with the TSPO Tracer [(11)C]PBR28. Molecular Imaging and Biology: MIB: the Official Publication of the Academy of Molecular Imaging 20(2):188–193. https://doi.org/10.1007/s11307-017-1129-z. PubMed PMID: 28983743.

[19] Vignal, N., Cisternino, S., Rizzo-Padoin, N., San, C., Hontonnou, F., Gele, T., et al., 2018. [(18)F]FEPPA a TSPO radioligand: optimized radiosynthesis and evaluation as a pet radiotracer for brain inflammation in a peripheral LPS-injected mouse model. Molecules 23(6). https://doi.org/10.3390/molecules23061375. PubMed PMID: 29875332; PubMed Central PMCID: PMC6099542.

[20] Wang, X., Minze, L.J., Shi, Z.Z., 2012. Functional imaging of brown fat in mice with 18F-FDG micro-PET/CT. Journal of Visualized Experiments: JoVE (69). https://doi.org/10.3791/4060. PubMed PMID: 23207798; PubMed Central PMCID: PMC3537196.

[21] Peres Valgas da Silva, C., Hernandez-Saavedra, D., White, J.D., Stanford, K.I., 2019. Cold and exercise: Therapeutic tools to activate brown adipose tissue and combat obesity. Biology 8(1). https://doi.org/10.3390/biology8010009. PubMed PMID: 30759802.

[22] Thyagarajan, B., Foster, M.T., 2017. Beiging of white adipose tissue as a therapeutic strategy for weight loss in humans. Hormone Molecular Biology and Clinical Investigation 31(2). https://doi.org/10.1515/hmbci-2017-0016. PubMed PMID: 28672737.

[23] Nakayama, A., Bianco, A.C., Zhang, C.Y., Lowell, B.B., Frangioni, J.V., 2003. Quantitation of brown adipose tissue perfusion in transgenic mice using near-infrared fluorescence imaging. Molecular Imaging 2(1):37–49. PubMed PMID: 12926236.

[24] Rice, D.R., White, A.G., Leevy, W.M., Smith, B.D., 2015. Fluorescence imaging of interscapular brown adipose tissue in living mice. Journal of Materials Chemistry B 3(9):1979–1989. https://doi.org/10.1039/C4TB01914H. PubMed PMID: 26015867; PubMed Central PMCID: PMC4442081.

[25] He, S., An, Y., Li, X., Wei, X., Sun, Q., Wu, Z., et al., 2018. In vivo metabolic imaging and monitoring of brown and beige fat. Journal of Biophotonics 11(8): e201800019. https://doi.org/10.1002/jbio.201800019. PubMed PMID: 29521002.

[26] Chondronikola, M., Beeman, S.C., Wahl, R.L., 2018. Non-invasive methods for the assessment of brown adipose tissue in humans. The Journal of Physiology 596(3):363–378. https://doi.org/10.1113/JP274255. PubMed PMID: 29119565; PubMed Central PMCID: PMC5792561.

[27] Ong, F.J., Ahmed, B.A., Oreskovich, S.M., Blondin, D.P., Haq, T., Konyer, N.B., et al., 2018. Recent advances in the detection of brown adipose tissue in adult humans: a review. Clinical Science 132(10):1039–1054. https://doi.org/10.1042/CS20170276. PubMed PMID: 29802209.

[28] Park, J.W., Jung, K.H., Lee, J.H., Quach, C.H., Moon, S.H., Cho, Y.S., et al., 2015. 18F-FDG PET/CT monitoring of beta3 agonist-stimulated brown adipocyte recruitment in white adipose tissue. Journal of Nuclear Medicine: Official Publication, Society of Nuclear Medicine 56(1):153–158. https://doi.org/10.2967/jnumed.114.147603. PubMed PMID: 25525187.

[29] Rosenwald, M., Perdikari, A., Rulicke, T., Wolfrum, C., 2013. Bi-directional interconversion of brite and white adipocytes. Nature Cell Biology 15(6): 659–667. https://doi.org/10.1038/ncb2740. PubMed PMID: 23624403.

[30] Altshuler-Keylin, S., Shinoda, K., Hasegawa, Y., Ikeda, K., Hong, H., Kang, Q., et al., 2016. Beige adipocyte maintenance is regulated by autophagy-induced mitochondrial clearance. Cell Metabolism 24(3):402–419. https://doi.org/10.1016/j.cmet.2016.08.002. PubMed PMID: 27568548; PubMed Central PMCID: PMC5023491.

[31] Rosenwald, M., Wolfrum, C., 2014. The origin and definition of brite versus white and classical brown adipocytes. Adipocyte 3(1):4–9. https://doi.org/10.4161/adip.26232. PubMed PMID: 24575363; PubMed Central PMCID: PMC3917931.

[32] Mizrahi, R., Rusjan, P.M., Vitcu, I., Ng, A., Wilson, A.A., Houle, S., et al., 2013. Whole body biodistribution and radiation dosimetry in humans of a new PET ligand, [(18)F]-FEPPA, to image translocator protein (18 kDa). Molecular Imaging and Biology: MIB: the Official Publication of the Academy of Molecular Imaging 15(3):353–359. https://doi.org/10.1007/s11307-012-0589-4. PubMed PMID: 22895910.

[33] Ghadery, C., Koshimori, Y., Coakeley, S., Harris, M., Rusjan, P., Kim, J., et al., 2017. Microglial activation in Parkinson's disease using [(18)F]-FEPPA. Journal of Neuroinflammation 14(1):8. https://doi.org/10.1186/s12974-016-0778-1. PubMed PMID: 28086916; PubMed Central PMCID: PMC5234135.

[34] Suridjan, I., Rusjan, P.M., Voineskos, A.N., Selvanathan, T., Setiawan, E., Strafella, A.P., et al., 2014. Neuroinflammation in healthy aging: a PET study using a novel Translocator Protein 18kDa (TSPO) radioligand, [(18)F]-FEPPA. NeuroImage 84:868–875. https://doi.org/10.1016/j.neuroimage.2013.09.021. PubMed PMID: 24064066; PubMed Central PMCID: PMC6283059.

